ARTICLE NO. 79-1309R

C 80-082

Combined Pressure and Temperature Distortion Effects on Internal Flow of a Turbofan Engine

00027
60001
60006

Willis M. Braithwaite* and Ronald H. Soeder†
NASA Lewis Research Center, Cleveland, Ohio

An experimental investigation was conducted to obtain an augmented data base for improving and verifying a computer simulation developed by an engine manufacturer. Data were obtained for combined 180 deg "square wave" distortion patterns of total pressure and total temperature imposed in various relative positions on a TF30-P-3 turbofan engine. The observed effects of the combined distortion are presented in terms of total and static pressure profiles and total temperature profiles at stations ahead of the inlet guide vanes as well as through the fan-compressor system. The profiles predicted by the multisegment, parallel-compressor simulation model were found to agree well with these data. The effects of relative position of the two components comprising the combined distortion on the degree of distortion required to produce surge are also presented. Certain relative positions required less combined distortion than either a pressure or temperature distortion alone, and these trends were satisfactorily predicted by the model.

Nomenclature

D	= inlet duct diameter
HPC	= high pressure compressor
IGV	= inlet guide vanes
L	= distance upstream of IGV
LPC	= low pressure compressor
max	= maximum pressure or temperature in profile
min	= minimum pressure or temperature in profile
N_1	= low rotor (fan) speed
N_{1R2}	= low rotor speed corrected to station 2
P_S	= static pressure
P_T	= total pressure
PCM	= parallel compressor model
R	= effective mean radius of IGV
RNI	= Reynolds number index, $\delta/\phi \cdot \sqrt{\theta}$
S	= stall point for PCM, Fig. 4
T	= total temperature
U	= unstall operating point for PCM, Fig. 4
v	= velocity
v_a	= axial velocity
WACR	= corrected core airflow
WATR	= corrected total airflow
β	= circumferential (yaw) flow angle
δ	= ratio of total pressure to sea level
Δ	= difference between numbers
θ	= ratio of total temperature to sea level
ϕ	= ratio of viscosity to sea level value

Subscripts

av	= average
A	= station A, downstream of screen
2-4	= stations in compressor
IGV	= IGV station
PCM	= parallel compressor model

Presented as Paper 79-1309 at the AIAA/SAE/ASME 15th Joint Propulsion Conference, Las Vegas, Nev., June 18-20, 1979; submitted July 5, 1979; revision received Dec. 10, 1979. This paper is declared a work of the U.S. Government and therefore is in the public domain.

Index categories: Airbreathing Propulsion; Engine Performance; Simulation.

*Head, Experimental Section B, Airbreathing Engines Division. Member AIAA.

†Aerospace Engineer, Engine Research Branch, Airbreathing Engines Division.

Introduction

THE effect of inlet flow distortion on the performance and stability of aircraft gas turbine engines has long been an important consideration in development programs. An extensive progam has been undertaken by the Lewis Research Center to evaluate the effects of inlet flow distortion on the various types of engines. This paper presents the results obtained with combined 180 deg square wave total pressure and total temperature distortions imposed on the inlet flow of a low bypass ratio turbofan engine.

The amount of experimental data required for the development of new engines may be reduced by use of analytical models of the compression systems. Such models should be capable of predicting the effects of distortions on compression system internal flow and stability. Preliminary estimates of distortion sensitivity can be obtained using the compressor design characteristics. As more experimental data are obtained the model becomes more reliable and thus reduces the uncertainties inherent in engine development.

Several such models have been developed by the engine manufacturers.[1-5] The model of the TF30[1] was fine tuned using total pressure distortion data generated during Lewis testing to match the particular characteristics of the engine being used.[6-8] This refined model was then used to predict the results of a proposed investigation of combined pressure and temperature distortions.

Development of these models require experimental data showing the characteristics of the flow into and through the compressor system. These characteristics include the usual pressure and temperature profiles. Also of interest is the direction and magnitude of the flow, or velocity vector, especially at the compressor inlet. Previous work has shown the effects of total pressure distortion on turbofan engines, and both pressure and temperature distortions on turbojet engines.[9-11] An experimental program was conducted using a TF30-P-3 turbofan engine to obtain better definition of the flow ahead of the inlet and through the compressor system. In addition, it was desired to evaluate the effectiveness of the model in predicting the flow characteristics with combined pressure and temperature distortions.

Apparatus

The TF30-P-3 turbofan engine used for this investigation was installed in an altitude test chamber at the Lewis Research Center. Two devices were used to generate the pressure and temperature distortions. The total pressure distortion was

generated with a 50% blockage screen mounted in the inlet duct approximately 1 duct diam ahead of the compressor face. The screen holder was capable of circumferentially indexing the screen and thus the distortion. The total temperature distortion was generated by means of the gaseous hydrogen burner mounted approximately 6 duct diameters ahead of the compressor face. The burner mounting permitted ±30 deg circumferential rotation of the burner. This movement, coupled with the indexing of the burning quadrants, permitted the indexing of the distortions in 30 deg steps.

The engine was instrumented in such a manner that circumferential profiles of total pressure and temperature and static pressure could be determined in front of and through the compression system. These profiles were measured just downstream of the distortion screen (station A), at the inlet guide vanes (IGV), and in the 1st, 3rd, 6th, 9th, 12th, and 16th stage stators. The location of each station is shown in Fig. 1. Two rows of static pressure taps extended from the distortion screen (station A) to the IGV and were located at approximately 120 deg from the top of the duct on the inner and outer annular walls.

Additional instrumentation was installed in the IGV to measure the angle between the flow vector and the axial direction. The instrumentation used was the five-point probe, described in Ref. 12, where the indicated pressure difference between the outer probes as a percentage of the approximate dynamic head is proportional to the flow angle.

The effect of combined pressure and temperature distortions on the stability limits was determined by slowly increasing the temperature distortion with the screen in place until stall was reached. Since the screen could be indexed independently of the burner, the effects of the relative position of the distortions could be investigated.

During the various phases of the investigation the following test conditions were maintained. The Reynolds number index (RNI) in the undistorted sector of the inlet was maintained at 0.5 with the temperature being 289 K. A low-pressure rotor speed of 90% of military and 100% rated jet nozzle area was used. A large amplitude pressure distortion was necessary to keep the distortion more discernible as it attenuated within the engine. Therefore, the 7th stage compressor bleed was open during the profile mapping but was closed for the stability limit part of the investigation.

Analytical Model

The compressor simulation used for the comparison of predicted results with the experimental data was a Pratt and Whitney Aircraft developed multiple segment, parallel compressor model. This model provides a detailed blade row by blade row circumferential definition of the distorted flowfield for the TF30-P-3 compression system by means of multiple parallel compressor segments passing through the compressor from inlet to exit. The flow rate in each segment is determined from its inlet total pressure and total temperature and exit static pressure. A uniform static pressure is assumed in the exit volume of each major unit. The performance of each segment is computed using the normal stage characteristics considering two-dimensional flow effects coupled with the unsteady flow resulting from the relative motion of rotor blades passing through the distorted regions. The model also computes the distorted flowfield entering the IGV using an exponential static pressure distortion buildup. This model and the simple parallel compressor theory are described in more detail in Refs. 1, 2 and 9,10, respectively.

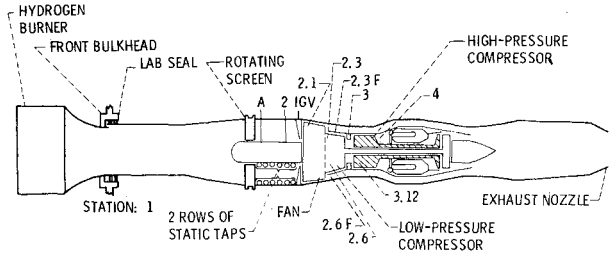

Fig. 1 Instrumentation layout for TF30-P-3 turbofan engine.

Results and Discussion

The effect of inlet flow distortion on the performance of a turbofan engine will be discussed in three sections. The first will describe the flow between the screen and the IGV; the second will describe the flow through the compression system; and the last will present the effects of the combined distortion and its orientation on the compressor stability limits.

Inlet Flow

For ease in describing the flows between the screen and the IGV, the effects of the total pressure and total temperature distortions will be treated separately. The parallel compressor theory requires a specific mass-flow profile at the engine face. But the flow behind the distortion screen did not match this profile as there was a rather severe flow distortion just downstream of the screen. As shown in Refs. 1 and 13, a static pressure distortion is generated by the attenuation of this flow distortion between the screen and the IGV.

The total pressure distortion generated by the 50% blockage screen is shown in Fig. 2. The 14% [(max-min)/av] total pressure distortion level was not attenuated between the screen and the IGV. However, the circumferential extent of the distortion was less at the IGV than just behind the screen. The static pressure distortion at station A was approximately 2% and increased to 9% at the IGV. Combining the total and static pressures and there being no total temperature distortion, the distribution of corrected mass flow per area was calculated and is shown in Fig. 2c. The mass flow distortion was about 60% at station A and decreased to 35% at the IGV.

The observed effects of the total temperature distortion are shown in Fig. 2d. In this case the total pressure distribution is uniform. It can be seen that the total temperature profile is not as square as was the total pressure profile. There appears to be an increase in temperature downstream of the plate dividing the two burning quadrants. The temperature distortion [(max-min)/av] at station A was approximately 32% and decreased only slightly at the IGV to 28%. There was almost no static pressure distortion at station A and only

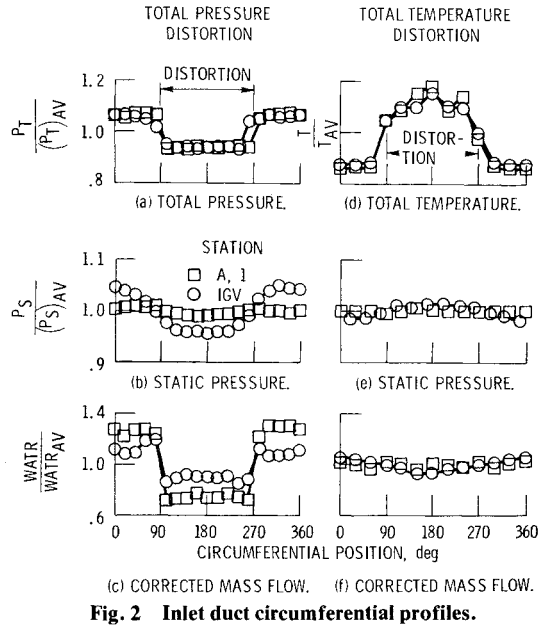

Fig. 2 Inlet duct circumferential profiles.

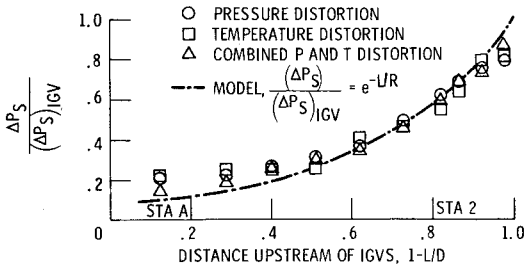

Fig. 3 Static pressure distortion on outer wall between screen and IGV.

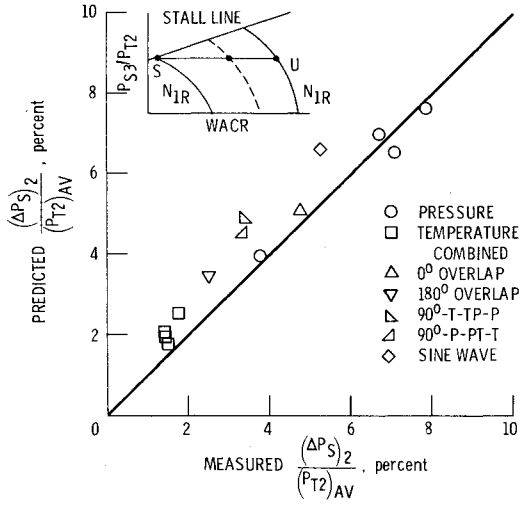

Fig. 4 Comparison of predicted and measured inlet static pressure distortion.

3% at the IGV. The resultant mass flow distortion was approximately 6% at station A and 12% at the IGV.

The buildup of static pressure distortion as the flow approaches the IGV was shown to follow an exponential relationship, as given in Refs. 1 and 13, for imposed total pressure distortions. The static pressure distortions resulting from total temperature and combined pressure/temperature distortions also follow this relationship, as indicated in Fig. 3 by the good agreement between the three sets of data. They are slightly higher than the exponential fit of the model near station A, but the levels of pressure are low and there is no effect of the distortion devices accounted for by the exponential fit.

One consequence of the static pressure distortion ahead of the compressor has been the apparent disagreement between the measured mass flow distribution and that predicted by the simple parallel compressor theory. This was especially true for the total temperature distortions. The insert on Fig. 4 shows a simple parallel compressor model representation of a temperature distortion. The flows for parallel compressor units S and U are significantly different. This difference would require a significant static pressure profile. The predicted static pressure distortion can be adjusted for the distance L_2 that station 2 is ahead of the IGV using the exponential relationship.

$$\frac{(\Delta P_s)_2}{(P_{T2})_{av}} = \frac{(\Delta P_S)_{IGV}}{(P_{T2})_{av}} \times e^{-L_2/R}$$

a modified version of the expression of Ref. 1. The results of this adjustment are shown in Fig. 4. The agreement is good for all the various configurations shown.

The angle that the flow makes with the axial direction at the IGV is shown in Fig. 5. This angle was measured ap-

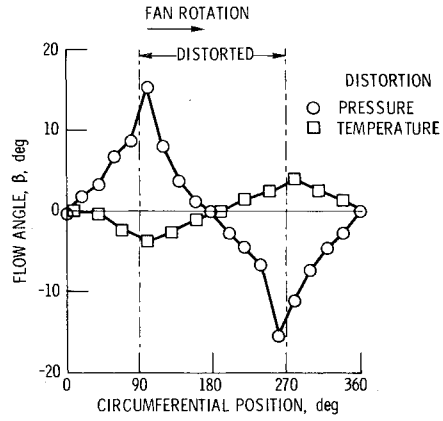

Fig. 5 Angle of distorted flow entering fan IGV.

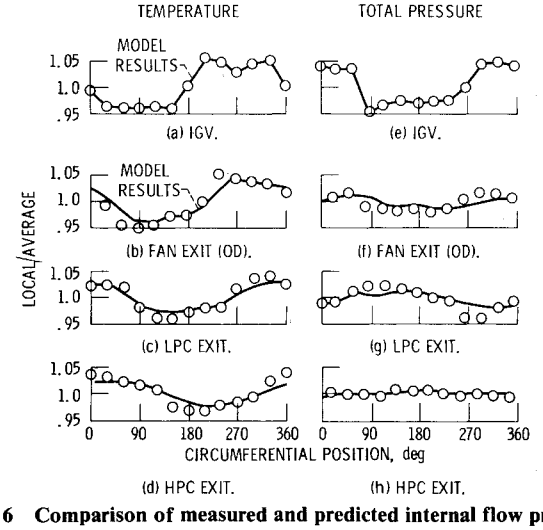

Fig. 6 Comparison of measured and predicted internal flow profiles for combined pressure and temperature distortions.

proximately 2.5 cm ahead of the IGV, about half way between the tip and the hub of the blade. The positive angle is defined as the one with a component in the direction of engine rotation. It can be seen that the total pressure distortion induced a positive flow angle at the leading edge of the distortion, or low pressure region, and a negative angle at the exit of this region. This implies that there is flow into the distorted region. From Fig. 2b it can be noted that this also is a region of low static pressure. For the total temperature distortions, the flow angle is negative at the leading edge and positive at the trailing edge of the heated section of the inlet. This is the reverse of that for the pressure distortion and implies that the flow is out of the heated region. The static pressure is higher in the heated sector, Fig. 2e, and, thus, the circumferential flow is again from the high to the low static pressure region. It can also be noted that the largest flow angle is in the region of the steepest total pressure gradient, that is, at the edge of the distortion, and the minimum angles are in the center of the distorted and undistorted regions where there is no total pressure gradient. The magnitude of the flow angle is much greater for the pressure distortion than for the temperature distortion. There is a 30 deg flow angle variation for the 14% pressure distortion and an 8 deg variation for the 28% temperature distortion. Compared on the basis of the static pressure distortions, there is a 30 deg variation for a 9% static pressure distortion associated with the total pressure distortion, and an 8 deg variation for the 3% static pressure distortion that is associated with the total temperature distortion. The flow angle, therefore, seems to be a function of the static pressure distortion.

Internal Flow

A combined total pressure and total temperature distortion was selected to demonstrate the capability of the model to describe internal flow characteristics. The 180 deg total pressure distortion was oriented in the lower half of the inlet, Fig. 6. The total temperature distortion was oriented such that the high temperatures were in the right hand side, Fig. 6. A compressor blade would thus pass through 90 deg of low temperature-high pressure followed by 90 deg of low temperature-low pressure, followed by 90 deg of high temperature-low pressure, and then 90 deg of high temperature-high pressure.

The fan inlet temperature and pressure profiles were then put into the multisegment parallel compressor model. The predictions from the program are represented by the lines on Fig. 6 for several key stages in the compressor. Reasonable agreement was achieved between the model and the experimental data. The predicted swirl or rotation of the center of both the total pressure and temperature distortions as they pass through the compressor can be seen here and in Fig. 7. This swirl can lead to some incorrect readings if it is not properly accounted for when specifying instrumentation for control sensors and/or research projects.

The TF30 model also predicted the inlet flow angles at the IGV, Fig. 8, and they are compared with the measured angles. The model predicted greater angles than measured in the undistorted regions with a maximum variation in the measured angle of 16 deg as compared to 19 deg for the model.

The measured attenuations of the total pressure and total temperature distortions and static pressure distortion are compared with those predicted by the model in Fig. 9. The experimental data exhibit a greater spread than does the model. However, the agreement was within 3.0% of the average temperature. The pressure distortions are attenuated as they pass through the compressor, decreasing from 9% to about 1% at the compressor exit. The total temperature distortion, however, was not attenuated to the same degree, going from 9% to 7%. The model had predicted a slightly greater attenuation to 5%.

The effects of relative position are shown in Fig. 10. The most persistent distortion occurs when the high temperature and low pressure are in the same 180 deg sector and the most attenuated occurs when they are opposed. The two 90 deg overlapping cases fit in between the extremes.

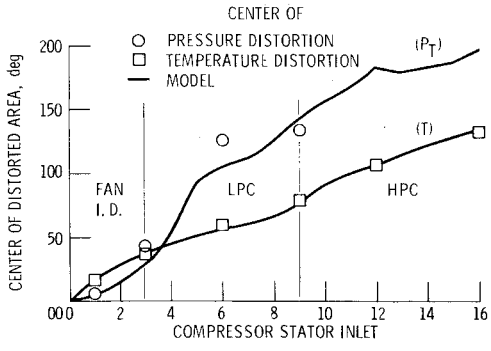

Fig. 7 Predicted swirl of total pressure and temperature distorted flow passing through compressor system.

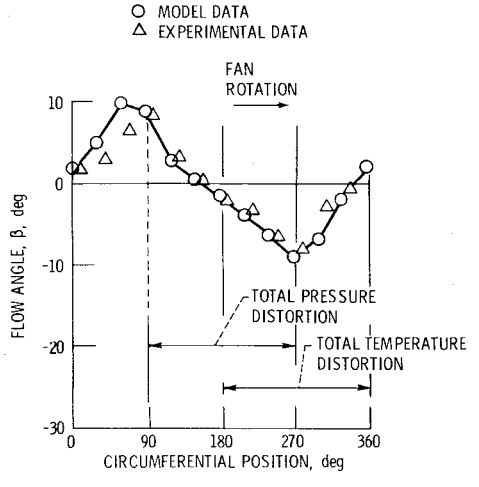

Fig. 8 Comparison of model and experimental approach angles for a complex flow distortion.

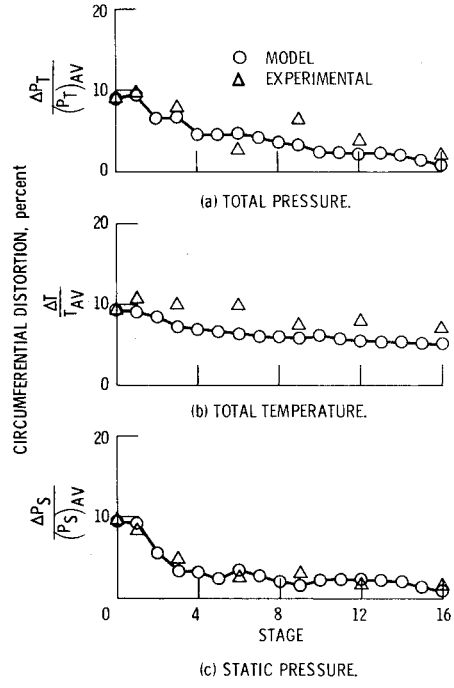

Fig. 9 Attenuation of distortion by compression system of combined *P* and *T* inlet distortions.

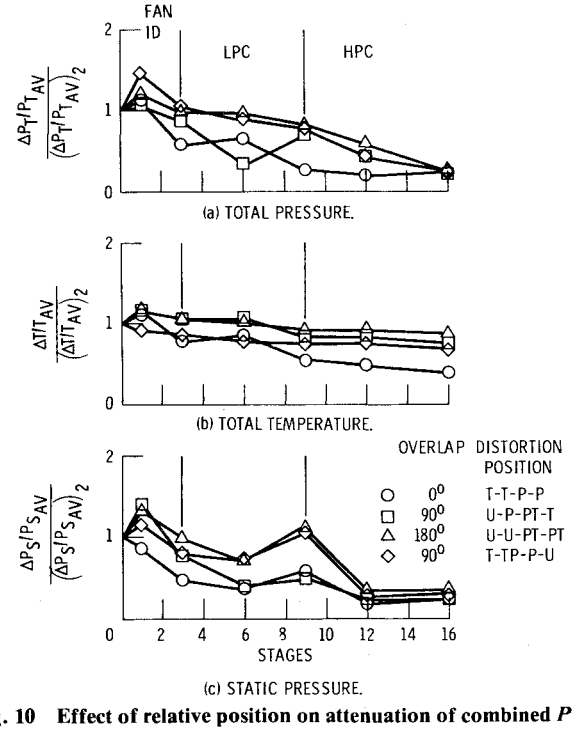

Fig. 10 Effect of relative position on attenuation of combined *P* and *T* distortion.

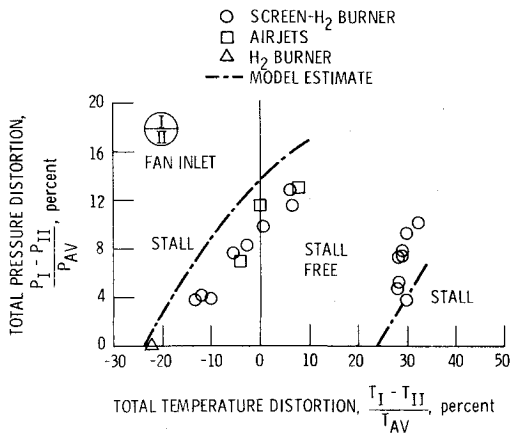

Fig. 11 Effect of relative position on limiting distortion for combined *P* and *T* distortions.

Stability Limits

The results of the experimental investigation into the combined distortions that resulted in compressor stall are presented in Fig. 11. Included on this figure are data obtained using airjets to generate the combined distortion. The amount of pressure distortion required to stall the compression system is shown as a function of various levels of temperature distortion. Two regions are shown on the figure; one in which the high temperature is aligned with the low pressure region (negative delta *T*), and one in which the high temperature and low pressure are opposed to each other (positive delta *T*). Starting with a negative delta *T*, pure temperature distortion, it is seen that as the temperature distortion decreases, larger total pressure distortions are required to stall the compression system until a pure pressure distortion is obtained. If the temperature distortion is now located in the opposite side of the inlet, increasing levels of pressure distortion are required for increasing temperature distortions.

A second limit line is observed for the opposed distortions. For a pure-temperature distortion, the distortion required to stall the engine is the same on either side of the engine. There is a stall region to the right of this point.

The analytical model[2] predicted the importance of the relative position of the low pressure and high temperature regions in the compressor inlet. The various trends observed were discussed in Ref. 9 using the simple parallel compressor theory. A near linear inverse relationship exists between the levels of critical distortions when the low pressure and high temperature zones are aligned. When the two distortions are opposed, two sets of critical values exist that result in stall. The upper limit line of Fig. 11 is where the pressure distortion results in stall and the lower line is where the temperature distortion causes the stall.

Several factors must be considered before determining the adequacy of the model. The experimental data were obtained at an inlet RNI = 0.5, whereas the model prediction was for an RNI = 1.0. Based on previous experience, this difference in RNI would result in the model overpredicting the distortion level by approximately 2% for both total pressure and total temperature. Thus, the experimental data and the predicted limits agree reasonably well considering the complexity of the T compressor, that is, one having a fan and low-pressure compressor on the same rotor spool. It is also difficult to accurately measure the temperature distortions due to the peaked profile as mentioned earlier. These peaks could be missed by the few rakes available during dynamic stability testing.

Concluding Remarks

Experimentally determined, distorted flow characteristics of the TF30-P-3 turbofan engine were compared to pretest predictions using the Pratt and Whitney Aircraft developed simulations. Results of this comparison were:

1) There was good agreement between the model and the total-pressure and total-temperature profile data.

2) There was good agreement on the static pressure distortion buildup between the screen position and the IGV.

3) The agreement between the measured and predicted flow angles at the IGV was satisfactory.

4) The model predicted the trends obtained with the combined pressure and temperature distortions at the limiting values. For aligned high temperature and low pressures, the pressure distortion required to stall the compressor increased as the temperature distortion decreased. For the opposed high temperature-low pressure case, the required pressure distortion increased as the temperature distortion increased. At higher temperature distortions, a lower limiting pressure distortion was found. The simple parallel compressor theory predicted this limit as the temperature dominated limit, the upper instability being the pressure dominated limit.

5) Indexing of the distortion past the instrumentation provided good resolution for the internal profiles.

References

[1] Mazzawy, R.S. and Banks, G.A., "Modeling and Analysis of the TF30-P-3 Compressor System with Inlet Pressure Distortion," Pratt and Whitney Aircraft, East Hartford, Conn., PWA-5302, April 1976; also NASA CR-134996.

[2] Mazzawy, R.S. and Banks, G.A., "Circumferential Distortion Modeling of the TF30-P-3 Compressor System," Pratt and Whitney Aircraft, East Hartford, Conn., PWA-5448, Jan. 1977, also NASA CR-135124.

[3] Mazzawy, R.S., Banks, G.A., and Weber, C.R. "Compressor Critical Response Time Determination Study," AFAPL-TR-76-45, June 1976.

[4] Tesch, W.A. and Steenken, W.G., "Blade Row Dynamic Digital Compressor Program. Vol. 1: J85 Clean Inlet Flow and Parallel Compressor Models," General Electric Co., Cincinnati, Ohio, R75AEG406, May 1976; also NASA CR-134978.

[5] Tesch, W.A. and Skeenken, W.G., "Blade Row Dynamic Digital Compressor Program. Vol. II: J85 Circumferential Distortion Model, Effect of Stator Characteristics, and Stage Characteristics Sensitivity Study," General Electric Co., Cincinnati, Ohio, R76AEG484, July 1978; also NASA CR-134953.

[6] Braithwaite, W.M., "Experimental Evaluation of a TF30-P-3 Turbofan Engine in an Altitude Facility: Effect of Steady-State Temperature Distortion," NASA TM X-2921, 1973.

[7] Evans, D.G., deBogdan, C.E., Soeder, R.H., and Pleban, E.J., "Some Comparisons of the Flow Characteristics of a Turbofan Compressor System With and Without Inlet Pressure Distortion," NASA TM X-71574, 1974.

[8] deBogdan, C.E., Dicus, J.H., Evans, D.G., and Soeder, R.H., "Effect of a 180° Extent Inlet Pressure Distortion on the Internal Flow Conditions of a TF30-P-3 Engine," NASA TM X-3267, 1975.

[9] Braithwaite, W.M., Graber, E.J., Jr., and Mehalic, C.M., "The Effect of Inlet Temperature and Pressure Distortion on Turbojet Performance," NASA TM X-71431, 1973; also AIAA Paper 73-1316, Nov. 1973.

[10] Graber, E.J., Jr. and Braithwaite, W.M., "Summary of Recent Investigations of Inlet Flow Distortion Effects on Engine Stability," NASA TM X-71505, 1974; also AIAA Paper 74-236, Jan. 1974.

[11] deBogdan, C.E., Moss, J.E., Jr., and Braithwaite, W.M., "Internal Flow Characteristics of a Multistage Compressor with Inlet Pressure Distortion," NASA TM X-3446, 1977.

[12] Dudzinski, T.J. and Krause, L.N., "Flow-Direction Measurement with Fixed-Position Probes," NASA TM X-1904, 1969.

[13] Plourde, G.A. and Stenning, A.H., "Attenuation of Circumferential Inlet Distortion in Multistage Axial Compressors," *Journal of Aircraft*, Vol. 5, May-June 1968, pp. 236-242.